

Synthesis of Patterned Vertically Aligned Carbon Nanotubes by PECVD Using Different Growth Techniques: A Review

Aparna Gangele^{†*}, Chandra Shekhar Sharma[‡], and Ashok Kumar Pandey^{†**}

[†]Department of Mechanical and Aerospace Engineering, IIT Hyderabad, Kandi, Sangareddy – 502285, Telangana

[‡]Department of Chemical Engineering, IIT Hyderabad, Kandi, Sangareddy – 502285, Telangana
Emails: me13p1006@iith.ac.in* and ashok@iith.ac.in**

Abstract

Immense development has been taken place not only to increase the bulk production, repeatability and yield of carbon nanotubes (CNTs) in last 25 years but preference is also given to acknowledge the basic concepts of nucleation and growth methods. Vertically aligned carbon nanotubes (VACNTs) are forest of CNTs accommodated perpendicular on a substrate. Their exceptional chemical and physical properties along with sequential arrangement and dense structure make them suitable in various fields. The effect of different type of selected substrate, carbon precursor, catalyst and their physical and chemical status, reaction conditions and many other key parameters have been thoroughly studied and analysed. The aim of this paper is to specify the trend and summarize the effect of key parameters instead of only presenting all the experiments reported till date. The identified trends will be compared with the recent observations on the growth of different types of patterned VACNTs.

In this review article, we have presented a comprehensive analysis of different techniques to precisely determine the role of different parameters responsible for the growth of patterned vertical aligned carbon nanotubes. We have covered various techniques proposed in the span of more than two decades to fabricate the different structures and configurations of carbon nanotubes on different types of substrates. Apart from a detailed discussion of each technique along with their specific process and implementation, we have also provided a critical analysis of the associated constraints, benefits and shortcomings. To sum it all for easy reference for researchers, we have tabulated all the techniques based on certain main key factors. This review article comprises of an exhaustive discussion and a handy reference for researchers who are new in the field of synthesis of CNTs or who wants to get abreast with the techniques of determining the growth of VACNTs arrays.



Aparna Gangele completed her Bachelor's degree from the department of Mechanical Engineering at Samrat Ashok Technological Institute (SATI), Vidisha, M.P., India in 2005 and the M.Tech degree in Mechanical Engineering from National Institute of Technology, Bhopal, India, in 2010. Currently, she is a Ph.D. research scholar at the Department of Mechanical and Aerospace Engineering in IIT Hyderabad. Her research interest lies in the field of micro & nano fabrication techniques.



Dr. Chandra Shekhar Sharma is an Assistant professor in the Department of Chemical Engineering at the Indian Institute of Technology, Hyderabad, India. Dr. Sharma received his B.Tech. in 2003 from Aligarh Muslim University, Aligarh followed by Ph.D. from Indian Institute of Technology, Kanpur in 2011, both in Chemical Engineering. His research interests are carbon based hierarchical materials, bio-inspired polymer functional surfaces, electrospun polymer and carbon nanofibers and carbon-MEMS. He has received many awards, including the DST Inspire Faculty Award (2015), INAE Innovative Project Award (2011) and Gandhian Young Technological Innovation Award (2014 & 2015). Dr. Sharma has 25 peer-reviewed publications in reputed international journals, including *Carbon, Langmuir, ACS Applied Materials and Interfaces, Small* and *Electrochimica Acta*. He has six patent applications filed and two book chapters to his credit.



Dr. Ashok Kumar Pandey is an Associate Professor in the Department of Mechanical and Aerospace Engineering at the Indian Institute of Technology Hyderabad. He received his B.E. degree in Mechanical Engineering from the Bhilai Institute of Technology, Durg, India, in 2001, and the M.S. and Ph.D. degrees in Mechanical Engineering from the Indian Institute of Science, Bengaluru, India, in 2003 and 2008, respectively. After completing his postdoctoral research at Technion, Israel, from 2008 to 2010, he joined IIT Hyderabad in 2010. He is the receipt of Hetenyi Award 2010 and best teaching award in 2012. His current research interest includes nonlinear dynamics, vehicle dynamics and micro and nanomechanics.

Keywords: Carbon Nanotubes (CNTs), Multi walled Carbon Nanotubes (MWCNTs), Single walled Carbon Nanotubes (SWCNTs), Vertically aligned Carbon Nanotubes (VACNTs), Chemical Vapor Deposition (CVD), CNT Growth Mechanism, CNT Precursor, CNT Catalyst.

Contents

1. Introduction.....	3
2. Carbon nanotubes- A time line	5
3. Patterned VACNT applications	5
4 Different Growth Techniques of Carbon Nanotubes	6
4.1 Arc Discharge	6
4.2 Laser Ablation.....	7
4.3 Chemical Vapor Deposition.....	7
4.3.1 Types of CVD	8
5. Features of different methods of Carbon Nanotube Production	10
5.1 Disadvantages of Arc Discharge and Laser Ablation	10
5.2 Advantages of Chemical Processes.....	11
6. Recent report on the growth of Vertical Aligned CNTs by Catalytic CVD method:	11
6.1 Catalyst	12
6.2 Substrates and buffer layers	12
6.3 Others.....	13
7. Conclusion and Perspective	15
ABBREVIATIONS	16
Acknowledgement	17
References.....	17

1. Introduction

A carbon nanotube is an atomic thick sheet of graphite (also known as graphene) which after rolling up becomes a hollow cylinder of diameter of the order of a nanometer. In the case of CNT nanostructure the length to diameter ratio exceeds 10000. This name is given due to their size because the diameter (till 0.7 nm) is of the order of few nanometers (approximately 50000 times smaller than the width of a human hair) but their length can be up to several millimeters [1, 2]. The multi walled carbon nanotubes (MWCNT) consisted of several consecutive graphitic shells separated by the distance of 0.34 nm. Nanotube diameters range is from ~0.4 to >3 nm for SWCNTs and from ~1.4 to at least 100 nm for MWCNTs [3, 4] with high length to diameter ratio.

The CNTs show unique electrical properties, extraordinary strength and very high conductivity for heat which provide tremendous potential for the use in many different applications in the field of structural, mechanical, thermal, optical, electrical & electronics, medicine and biomedical etc.

The patterned and vertical aligned CNTs are required in many applications such as single-molecular transistors in microelectronics and electron emitting flat panel displays where the remarkable properties of individual CNTs can be easily and effectively used in devices, few more potential applications are

catalysts for fuel cells, connectors for electrical and thermal managements, membranes for chemical and biological separations, chemical and biological sensors, smart fibers and films for flexible optoelectronics, and even dry adhesives mimicking gecko foot etc.

Many fascinating optical properties are observed in VACNT arrays such as high absorptivity [5, 6], polarization-dependent reflection and wavelength-selective emission [7, 8], directional emission [9], photonic crystal effects [10, 11]. These properties of VACNT array depend on the orderly arrangement of the CNTs which includes pattern and intertube distance. Also the use of vertically aligned arrays of nanotubes and nanowires has been demonstrated in photonic crystal [12], solar [13, 14], nanoantenna [15] and mode-locked fiber lasers [16] applications. In case of nanoelectrode array [17] and field emission [18, 19] applications maintaining the areal site density of VACNTs is an important consideration due to the electric field shielding effects resulting from closely packed arrays of CNTs [20, 21]. The processes to pattern the catalyst such as photolithography [22, 23], electron-beam lithography, ink-jet printing [24, 25], microcontact printing [26, 27], electrochemical deposition [28] and self-assembly [29] are used to decrease the areal site density of CNT arrays by pre-patterning the catalyst site density for further growth of patterned and aligned CNTs. To enhance the production rate of patterned VACNT arrays the use of inkjet printing for catalyst deposition is more desirable instead of conventional photolithography or electron beam lithography patterning techniques.

The patterned and aligned CNT arrays weakens the electric field shielding effect and improves the distribution of electric field. The patterned CNTs are suitable for ordered arrays of CNTs emitters. The process to grow these is compatible with silicon integrated circuit processing and it incorporates such arrays into some photoelectric devices.

The concerns in this field are the reproducibility, fabrication of large scale quantity, controllability of length, diameter, chirality and intertube spacing or areal density, particular growth at selective

location including its applications at nanoscale devices i.e. electrodes for secondary batteries, fuel cells, memory devices and field emission displays etc.

2. Carbon nanotubes- A time line

The concise list of yearly important incidents and corresponding publications in the field of carbon nanotube growth, properties and its corresponding applications are tabulated in **Table 1**.

3. Patterned VACNT applications

Large availability of SWCNTs make it useful in many structural applications due to its low weight and high strength. In CNT based nanoelectronics SWCNTs have been investigated for transistors and diodes. Tans [30] and Martel et al. [31] demonstrated fabrication of SWCNTs by laser ablation and transplanted into the gap between the drain and source contacts in transistors, where the horizontal growth of CNT across two contacts was done which is against the natural growth direction (i.e. vertical). Arrays of CNTs are used in many applications like gas separation, gas absorption and as catalyst support. In the areas of energy storage applications CNTs are used to store metal (e.g. Li ion) and gas (e.g. H₂) molecules [32]. In silicon IC manufacturing SWCNTs and MWCNTs are used as interconnects due to the high thermal conductivity of the CNTs making them suitable in dissipating the heat from the chips and for their high current carrying capacity which is more than 10^7 A cm⁻².

The application of MWCNT tips has demonstrated the mapping of the shape and depth of holes, grooves and trenches in IC manufacturing for profilometry [33]. This requires the active development of scaleup techniques to synthesize the hundreds of CNT tip cantilevers on a substrate or wafer compared to the single and batch production. PECVD has a potential to be an ideal method to enhance the quantity, provide the desired orientation by maintaining the material quality. All the remarkable properties of individual CNTs can be easily and effectively assessed by patterned and vertical aligned CNTs in devices.

The MWCNTs and MWCNFs on patterned substrates has many applications in the field emitters which are used in flat panel displays for computer screens, television and large outdoor displays [32]. ACNTA electrode are regularly aligned and equally spaced CNTs which allows the electrode to possess large pore size and a regular pore structure as compared with the ECNT electrode. ACNTA electrode exhibits higher specific capacitance, superior ion diffusivity and better rate capability.

ACNTA electrode shows much higher electronic conductivity than ECNT electrode. Therefore, ACNTA electrode has much lower equivalent series resistance (38.1Ω) than ECNT electrode (88.9Ω) [34]. This behavior opens the field of batteries applications such as the aligned MWCNTs on the stainless-steel (SS) substrate obtained by CVD technique can deliver an initial capacity of 132 mAhg^{-1} at $1C$ rate and a reversible capacity of 460 mAhg^{-1} after 1200 cycles with the specific capacity increased about 250% in spite of the morphology of the MWCNTs with surface and structural defects and the SS substrate [35]. Patterned vertically aligned MWCNTs are suitable as electrodes due to large surface area and pore structure responsible for improved electrolyte accessibility, superior ion diffusion and charge transport capability. An array of such MWCNTs reinforced with SiO_2 in the space between individual tubes for mechanical stability and isolation [36]. Such type of array can also be used for the development of infrared detectors and the space filled arrays demonstrated to be used in biosensor development where DNA is attached to individual tube ends [32, 37].

4 Different Growth Techniques of Carbon Nanotubes

CNTs have been synthesized in large quantities for industrial applications. CNTs have been synthesized mainly by arc discharge, laser ablation and chemical vapor deposition (CVD) [38] etc. All these methods take place with the process gases or in vacuum. These three techniques will be discussed here.

4.1 Arc Discharge

Initially in 1980 the arc-discharge technique was used to synthesize carbon nano-onions [39] and Buckminster fullerenes in 1985 [40]. In this process, the carbon is contained in the negative electrode which sublimates due to the high discharge temperature which is above 1200°C . Iijima (in 1991) synthesized MWCNTs in the carbon soot of graphite electrodes with 100 A current [41]. By suitable arc-evaporation conditions bulk quantities of MWCNTs can be produced [42]. SWCNTs were also synthesized by using catalysts [43, 44] and in massive quantities [45]. The CVD method has been most widely used for CNT synthesis and elaborated in various literatures [37, 45, 46]. The diameter and the length of the CNTs are hard to control because of the pressure and temperature variation problem [46]. The length of both SWCNTs and MWCNTs can be produced up to $50\mu\text{m}$.

The yield is up to 30% by weight which is low and the process for purification is difficult, but CNTs have good crystallinity and lesser structural defects. So this method is widely adopted. The production of SWCNTs can be done on large scale by the electric arc-discharge process [45].

It was reported that self-aligned CNTs were produced [47] using copper catalysts in the soot deposited at the carbon cathode by a DC arc discharge method. These aligned CNTs have average diameter of about 400 to 600 nm.

The process of producing arrays of MWCNTs from a methane-hydrogen gas mixture activated through DC discharge without catalyst has been also been shown in some experimental setups [48]. It is seen that the hydrogen plasma promotes the nanopores formation in silicon substrate. The important inner pore surface are used as a mask in the formation of aligned nanotubes.

4.2 Laser Ablation

Laser ablation is a process to irradiate the surface and remove materials from a solid surface with the help of laser beam. The solid material is heated by the absorbed laser energy at low laser flux for sublimation or evaporation. CNTs were synthesized by Laser ablation in 1995 [38, 49, 50].

A simple schematic diagram for this method is shown in **Figure 1**, where to grow the CNTs a graphite block is used inside a chamber that is irradiated using a pulsed laser, followed by flow of Argon along the laser. The temperature of the chamber is approximately 1200⁰C. The laser ablates the graphite target and thus carbon is vaporized, condensed and collected on a cold copper collector due to flowing Argon gas. A water cooled surface can also be used to collect the CNTs.

The metal catalyst particles (cobalt and nickel) and a composite block of graphite can be used to produce SWCNTs [49] and a pure graphite can be used as the starting material to produce MWCNTs [50]. The problem in this process is that carbon layer completely covers the catalyst particles so no further atoms of carbon can be deposited and the growth of CNTs is inhibited.

The reaction temperature is the key parameter to control the diameter of CNTs which made it costlier than arc discharge and CVD because of the high-power lasers. Although other heating methods can also be used, i.e. an electron beam [51, 52]. Patterned CNTs can also be produced by this method. The yield is around 70–90% by weight for MWCNTs [53].

4.3 Chemical Vapor Deposition

Chemical vapor deposition (CVD) is a chemical process providing high performance and purity of produced materials. Thin films are made by this method usually in semiconductor industry. The CVD method is widely used due to easy setup and lower cost. In 1959, the catalytic vapor-phase deposition of carbon was done on Fe using carbon monoxide and hydrogen mixtures [54]. In 1993, CNTs were produced on Fe particles using acetylene at 700⁰C by this process [55]. The aligned CNTs which

were approximately perpendicular to the surface produced on mesoporous silica using iron nanoparticles as catalyst by thermal CVD in large scale [56].

The very long aligned MWCNTs which were approximately perpendicular to the surface on the silica substrate fabricated and made an array of tubes with spacing of about 100 nm and height of approximately 2 mm [57].

The aligned CNT bundles were also produced on thin films of a cobalt catalyst patterned on a silica substrate by the CVD method [58]. The MWCNTs can be produced on catalyst patterns embedded on silicon substrate by a base growth mechanism using different mask techniques [58].

CVD is the simple process by which CNTs can be directly grown on a specified substrate. Large scale synthesis of CNTs are commercially possible with CVD method because of its lower price per unit ratio.

4.3.1 Types of CVD

There are so many types of CVDs that are possible. A substrate is deposited with a layer of metal nanoparticles as catalytic e.g. Ni, Co, Fe, or a combination of these metals in the thermal CVD or PECVD process. The arrays of vertically aligned CNT with invariable length and diameter usually have well marked specific properties and are being fabricated on different patterned substrate surfaces by thermally or plasma driven chemical vapor deposition (CVD). The thermally or plasma driven CVD process require carbon source as hydrocarbon precursor molecules (methane, acetylene, ethane etc.) and metal particulate iron, nickel and cobalt as catalysts to grow the arrays of high density on different substrates. Broad classification of CCVD is Thermal CVD and Plasma enhanced CVD. Further Temperature based CVD is divided into (i) Single step Method (Floating Catalyst CVD) and (ii) Double step Method (Water assisted CVD, Alcohol catalytic CVD, Thermal CVD) while the Plasma based CVD is categorized as Water assisted plasma CVD, Plasma assisted CVD (Direct current PECVD, Radio frequency PECVD, Diffusion PECVD, Microwave PECVD).

The growth temperature for CVD is about 600-950⁰C which is lower than the temperature in arc-discharge and laser ablation processes. Further plasma is used to reduce the temperature in CVD method compared to the thermal CVD. Plasmas are used to force reactions that would not be possible at low temperature. Moreover, CNT array grown by thermal CVD method is curly but the CNT array grown by a PECVD method is highly aligned to the vertical direction. Plasmas can be used to perform low temperature deposition of materials which are not possible thermally due to their low thermal energy. When fast diffusing metals like copper are used, this low temperature deposition becomes more important.

The PECVD method is the most promising method in which the carbonization of the precursor gas is done by the generation of a DC or RF plasma [60] to produce MWCNTs and SWCNTs, arrays of MWCNT [56, 58] and patterned SWCNT strands [61] on different substrates. The arrays of CNTs were grown on glass by employing plasma at 660⁰C [62]. The temperature can be reduced to 300⁰C with the various plasma techniques. Sometimes this method further facilitate the fabrication of CNTs at very low temperatures till 150⁰C over large substrate areas [63, 64], which makes it more widely acceptable and applicable than the other CCVD synthesis techniques [65–67].

The experimental set up of PECVD is set of equipment to handle and control the process and also to increase the overall efficiency of the process. The main components of PECVD experimental set up are rotary pump to reach a pressure of 10⁻² Torr, turbo molecular pump to get a pressure of 10⁻⁶ Torr, mass flow controller to measure the flow of carbon source, etching or reducing gases, vacuum gauge to measure the pressure inside the chamber, heater to get temperatures up to 900⁰C and its controller, reaction or vacuum chamber to withstand high temperature and accommodate the cathode chuck on which a substrate is set and anode is on top side, plasma power supply to generate the plasma, Plasma was formed between anode and cathode by applying a DC or RF voltage and other fittings for gases and water flow and their control.

The metal catalytic nanoparticles can be generated by other means also, like oxides solid solutions or reduction of oxides. The masked or patterned deposition of the metal, annealing or by etching with plasma of a metal layer are used to control the size of the metal catalytic nanoparticles. The temperature to heat the substrate with catalytic particles is approximately 700⁰C in a protective environment. Two gases are supplied into the chamber, a process gas e.g. ammonia, nitrogen or hydrogen and a carbon source gas e.g. acetylene, ethylene, methane or ethanol to grow CNTs on the metal catalyst.

Initially the carbon source gas is broken apart at the surface of the metal catalytic nanoparticles and the detached carbon is flown to the edges of the metal catalytic nanoparticles and this carbon forms CNTs. It depends on the adhesion between the substrate and the metal catalytic nanoparticles that it will remain at the nanotube bases or at the tips of the growing nanotubes in the growth process. The diameters of the grown nanotubes are affected by the size of the metal catalytic nanoparticles.

In CCVD synthesis process the uniform diameter of the carbon nanotubes is affected by the size of the catalyst particles. These catalyst particles can be deposited in systematic and even complex pattern of arrays to fabricate well aligned CNT bundles, forests or assemblies [56, 58]. The CPECVD process can control the alignment, geometry, structure and site of CNTs. The major steps involve

usually for the growth of vertical aligned CNTs on patterned metal catalyst by PECVD are basically three steps of the VLS mechanism:

- 1.) Decomposition of the carbon source gas or precursor on the surface of catalyst particle.
- 2.) Diffusion of carbon atoms through the bulk and surface of the catalyst as a solid solution.
- 3.) Precipitation of carbon atoms beneath the catalyst or at the metal-substrate interface, subsequently growth of CNT.
- 4.) Another possible mechanism is that carbon atom diffuse only on the surface of the catalyst particle.

The vapor-liquid-solid mechanism represents the steps for the growth of CNTs by PECVD using metal catalyst thin film. Initially catalysts are deposited on the substrate then the substrate is heated to a particular temperature and catalyst layer melts and starts to form liquid droplets. These droplets forms a eutectic alloy by absorbing the vapor and become supersaturated with the carbon source vapor and carbon precipitates and CNTs starts growing. The continuous supply of the vapor is responsible for vertical alignment of CNTs.

5. Features of different methods of Carbon Nanotube Production

Both arc discharge and laser ablation methods suffer from disadvantages of being expensive and uneconomical for production of carbon nanotubes on large scale, although they yield high quality CNTs with reasonable high yield. CVD is best suited, economic method of production of high purity SWCNT on large scale. **Table 2** shows the concise comparison of different methods to grow CNTs.

5.1 Disadvantages of Arc Discharge and Laser Ablation

The Arc Discharge and Laser Ablation both methods generates the high quality nanotubes but having some disadvantages which bounds their use in large scale industries for mass production of CNTs.

- 1.) The solid carbon or graphite is used as a target which is evaporated and produces nanotubes after condensation in both the specified methods. In large scale process it is hard to get such a huge graphite as target which restricts their being used as industrial process.
- 2.) A huge amount of energy is required to produce arc or laser in Arc-Discharge and Laser ablation processes respectively, so these are the energy extensive methods. Such a large amount of energy is difficult to provide for large scale production and makes them a costlier process.
- 3.) The CNTs generated by both the above methods are highly entangled and having undesirable form of carbon and sometimes catalysts also. So post treatment processes are required to purify and assemble the produced forms which makes the processes again costlier and difficult.

5.2 Advantages of Chemical Processes

These methods have many advantages as compared to above mentioned processes.

- 1) The process is cheap in terms of unit price, because there is no need of expensive and hard to produce targets. Huge amount of energy is also not required.
- 2) The design of the reactor and reaction process is simple and the reaction is easy to handle or control.
- 3) Raw materials in bulk are easily available in the gaseous form required for reaction processes.
- 4) This process is distinctive in synthesis of VACNTs and no other process are capable to produce such aligned nanotubes.

This process can synthesize CNTs directly on different substrates which makes the process simple by eliminating the collection, separation and transfer steps. The post refining processes are not always required to some extent. Although some refining or functionalization step are required in some cases for further purification and desired applications.

6. Recent report on the growth of Vertical Aligned CNTs by Catalytic CVD method:

Table 3 summarizes the comprehensive current report of the different process parameters and their effects on the growth of Vertical Aligned CNTs by catalytic CVD synthesis method.

One of the most adopted process steps represents the vapor-liquid-solid mechanism to grow patterned VACNTs by PECVD method. Initially catalysts are deposited on the substrate then the substrate is heated to a particular temperature and catalyst layer melts and starts to form liquid droplets. These droplets forms a eutectic alloy by absorbing the vapor and become supersaturated with the carbon source vapor and carbon precipitates and CNTs starts growing. The continuous supply of the vapor is responsible for vertical alignment of CNTs. Different steps of photolithography such as cleaning, drying, spin coating, soft baking, photomask, exposure, developing and cleaning have to be optimized. These optimized parameters are used for patterning the catalyst nanodots on substrate to fabricate the arrays of CNTs. Depending on the cohesion between the interlayer of catalyst metal and buffer layer or substrate varying thickness of catalyst is deposited and further lift off is done. CNTs are grown on the particular sites as formed by patterning. The example of using inkjet printing to synthesis the high yield VACNT forests grown at particular sites on the substrate is shown in **Figure 2** with CNTs length of 400 μm .

6.1 Catalyst

The catalyst is one of the major factors of CNT growth in the CVD process. Melechko et al. has summarized some catalysts used for CNT growth [68]. The catalysts like nickel [22, 51, 68–73], cobalt [74–78], iron [56, 59, 79–81], stainless steel [82–84], gold [85], platinum [80] and their alloys are used successfully and effectively.

There are many formation mechanisms proposed for catalytically grown CNTs in the literatures [86–92], e.g. surface diffusion mechanisms [87], bulk diffusion mechanisms [86, 93], spatial velocity hodograph [88] and catalyst surface step edge effects [89]. There is also a two-step growth mechanism- the first step is the catalytic growth of a CNT and the second step is thickening step with the catalyst free pyrolytic carbon deposition mechanism [94–98].

In the growth of VACNTs by CVD, carbon source such as hydrocarbon (e.g. methane, acetylene, ethylene, naphthalene, benzene, etc.) pyrolyzes over metal catalysts (i.e. Pd, Fe, Co, Ni, and Pt) and deposited on different substrates. Various pyrolytic CNT growth mechanisms are described in the literatures [86, 94, 99–102]. Some of the example of growing patterned VACNTs including one such work done at University of Cambridge are demonstrated in **Figure 3**. The following three mechanisms of the pyrolytic CNTs growth have been widely recognized in recent times-

- (1) Bottom carbon diffusion through catalytic particles.
- (2) Surface carbon diffusion on catalytic particles.
- (3) Top carbon diffusion through catalytic particles.

6.2 Substrates and buffer layers

A strong solid base is provided by a substrates for growing patterned VACNTs. The morphology of the formed VACNTs is decided by the lattice matching. In order to resist the agglomeration the substrate should be capable to prevent the mobility of the catalyst particles. Alignment, density and diameter are controlled by changing the structural morphology of the substrate. Silicon is not an ideal substrate even though silicon wafers are one of the most popular and widely used substrates studied to synthesize VACNTs. The surface of a silicon wafer is anodized and made porous to control the density and diameter of the catalyst particles as reported by Lee et al. [103]. ACNTs are grown successfully on 1D and 2D Si substrates with porous AAO nanotemplates by Li et al. [104, 105].

Catalyst support also known as the adhesion layer, buffer layer or underlayer is always used to isolate silicon from active catalysts and restore its activity. Buffer layer also increase the surface roughness

for better adhesion of catalyst nanoparticles and enhances the dispersion of catalyst nanoparticles on the substrate surface [106].

The interaction between the plain silicon wafers with Fe as a catalyst in CVD is studied by Jung et al. [107]. They found that Fe reacted and formed iron silicide (FeSi_2) and iron silicate (Fe_2SiO_4) with silicon at high temperatures. FeSi_2 and Fe_2SiO_4 are non-catalytic to grow the CNTs and a similar phenomenon also occurs in case of using Ni and Co. A layer of SiO_2 is proved as an ideal catalyst support to grow VACNTs due its high surface roughness [108]. This layer isolates the interaction of catalyst with silicon substrate. Sometimes SiO_2 is used with Al or alumina also. SiO_2 is used to lower the reaction between Al with Si before alumina is formed but if the aluminium oxide layer is too thick, it will bury the catalyst particles and constraint the growth of CNTs. Although the growth of VACNTs can be enhanced by increasing the thickness of the Al buffer layer [109]. Al and Alumina is used to avoid extensive sintering of Fe particles [110]. The use of Al increased the growth rate and morphology of CNTs as found by Liu et al. [111] and lessen the oxidation of catalyst on the catalyst surface which helps in restoring the catalytic activity as reported by Vander et al. [106]. An alloy of Al and another catalysts can also be made to promote the activity of the catalyst [111]. The adhesion layers of Tantalum and Tungsten-Ti bimetals are used to reduce the diffusion of Ni particles into the substrate [112]. Titanium nitride is another example [113].

A quartz tube is directly used as a substrate to grow VACNTs in FCCVD. So the Quartz is another substitute of silicon often used as a substrate. Al_2O_3 fibre cloth [114], Alumina–mullite mixtures, MgO, sapphire [115], and machinable ceramic [111] are another important substrates for growing ACNTs. In the sol-gel method, mesoporous silica thin films are used. The preparation conditions of the iron/silica substrate are responsible for a specific diameter and distribution of VACNTs [116, 117]. Ceramic spherical substrates are proposed for mass production of ACNTs because a flat substrate has a low surface area for the growth of CNT arrays [118, 119]. Lamellar Fe/Mo/vermiculite is used successfully in fluidized bed-CVD for mass production [120].

6.3 Others

Several literature has shown that the growth of VACNTs depends on parameters such as catalyst film thickness, substrate temperature, gas ratio of carbon source gas and reducing gas, pre-treatment using plasma and growth time [28, 66, 121–123].

Catalyst thickness: The catalyst particle size depends on the initial catalyst layer thickness, the underlying surface, the annealing temperature and diameter of the deposited catalyst material. An increasing CNT height with increasing catalyst volume is observed. The temperature varies the

surface energies, but due to high temperature, larger islands can be formed due to Ostwald ripening effect. A higher anneal temperature can also promote the formation of silicides which will affix the catalyst and ensure base growth. The varying thickness of post-annealed deposited Ni catalyst films is shown in **Figure 4**.

Temperature: At higher temperatures the carbon source gas dissociates faster. A higher diffusion rate of carbon atoms through the catalytic particle results in considerably longer CNTs. However, as the deposition temperature is increased further till 900⁰C, the CNTs become disordered, entangled or loses alignment. The nanotube deformation at 900⁰C may be due to ion damage caused by higher plasma ionization. The nanotubes grown near by 700⁰C are usually well-aligned and uniform in size. The growth rate at 550⁰C is much less may be because of insufficient nucleating nanotubes, inadequate to decompose carbon source gas, limiting the graphitization consequently hindering growth. The lower deposition temperature is responsible for low growth rate instead of lack of plasma density because the thermal growth occurs without any plasma at 700⁰C [124].

Gas ratio: The gas mixture which control the CNT morphology is optimized to minimize any amorphous carbon deposition onto the unpatterned areas with the help of reducing or etching gas. The function of reducing or etching gas is to etch the by-products such as amorphous carbon and graphitic phases keeping the gas side of the catalyst particle free from carbon and allowing the continuous access of gas to the catalyst, so that it remains activated throughout the growth process of CNT. Etching is an important aspect of growing well oriented nanotubes with uniform diameters from top to bottom.

The growth changes dramatically from nanotubes to tip structures for variable quantity of carbon precursor gas flow. As higher concentration of feed gas in the plasma compensates for the etching by reducing gas, the initial rise in nanotube length is expected. The carbon diffuses through the metal particles and precipitates below it at high carbon source gas flows. But the vertical nanotube growth cannot be continuing with the amount of carbon extruded through the metal catalyst, at concentrations over 50%, so the pyramidal structures, cauliflower-like structure are formed.

Pressure: Growth rate increases with higher pressure of the process gases due to increased density of hydrocarbon gas near the catalytic particle, but higher pressure also causes faster back etching of the CNTs. The nanotube length increase with gas pressure, while the gas ratios are kept constant.

Power: The alignment of the CNTs depends on the electric field and the electric field of order of 0.1~1.0 V/mm is necessary to align the nanotubes. The applied voltage controls the plasma properties

(such as the bias current, degree of ionization/excitation) if conditions such as pressure and electrode gap are kept constant.

CNTs are better aligned at high power, but rate of etching enhances due to strong ion bombardment. The growth rate decreases with increasing power because the carbon source gas already decomposes in the plasma instead of at the catalyst surface. These free carbon species are not responsible for the CNT growth.

Growth time: CNT length is expected to depend linearly on the growth time. Thus the growth rate is maximized by minimizing the particle size, and the particle size controls both nanotube diameter and growth rate.

7. Conclusion and Perspective

Different techniques and fabrication processes used to grow VACNT arrays have been discussed and reviewed. Many processes have been explored to fabricate VACNTs, every process has its own limitations. A number of different smart materials and advanced devices are possible to develop via various multifunctional patterned VACNTs by controlled CNT growth and their ordered pattern along with some chemical and structural modification of the constituent nanotubes. However out of all the techniques no one is practically meeting the criteria such as an ease of high speed and bulk production, cost effectiveness and keen control of process. As VACNT structures have many potential applications when grown by PECVD, so the development in this area is gaining a lot of importance even though commercialization of large scale production processes with successful applications depend on understanding and controlling of several key parameters. These parameters are interdependent and makes the synthesis of VACNTs more complex and challenging. Furthermore the preparation of the catalyst which is used to synthesize VACNTs is even more complicated. Consideration needs to be given to the combination of the catalyst, catalyst support and substrate. The research on the fabrication and applications of VACNTs is ongoing and still there are many mysteries and challenges waiting to be answered and discovered, some of which are mentioned for e.g. type of materials that are used for the growth of VACNTs, avoiding the undesired radicals which increase the contamination by amorphous carbon, in place of CNTs without harming the vertical alignment how amorphous carbon only should be etched away.

Some points which needs keen analysis for more control of the process and better reproducibility of the VACNTs are the particular role of ions and dependence of ion energy for the growth of VACNTs and the effect of ions to loose the particle adhesion to the surface, the role of atomic hydrogen and the

role of preferable hydrogen-carrying diluent (Hydrogen, Ammonia, Argon or Nitrogen), the effect of the different types of metal Catalytic nanoparticles, its size, method of deposition, thickness of the layer, pretreatment process on the growth rate and the diameter of the CNTs and areal density of the VACNT arrays, the possible process parameters to grow specifically SWCNTs or MWCNTs patterned arrays by PECVD method with minimum possible defects.

Future challenges regarding the controlling parameters to grow patterned VAMWCNTs by PECVD method are the process parameters responsible for Tip or base growth, steps which determines the growth rate of VACNTs, mechanism for vertical or horizontal alignment, the effect of electric field in orientation and alignment of growth, in hot-filament, resistive heating, IR lamp etc. which heating method is better to heat the substrate, the minimum possible temperature for growth e.g. for glass substrates, the maximum appropriate value of dc bias and the effect of it on the CNT structure, growth rate and alignment, the effect of pressure along with the effect of other process parameters will have to be surely known.

Thorough analysis and clear understanding of the above mentioned points are beneficial for the future development in the respective field.

ABBREVIATIONS

CNT: Carbon nanotube

VACNT: Vertically aligned carbon nanotube

ACNTA: Aligned carbon nanotube array

ECNT: Entangled carbon nanotube

MWCNT: Multi-walled carbon nanotube

SWCNT: Single-walled carbon nanotube

HACNT: Horizontally aligned carbon nanotube

VASWCNT: Vertically aligned single-walled carbon nanotube

VADWCNT: Vertically aligned double-walled carbon nanotube

VAMWCNT: Vertically aligned multi-walled carbon nanotube

CCVD: Catalytic chemical vapor deposition

PECVD: Plasma-enhanced chemical vapor deposition

ACCVD: Alcohol catalytic chemical vapor deposition

WACVD: Water-assisted chemical vapor deposition

TCVD: Thermal chemical vapor deposition

FCCVD: Floating catalyst chemical vapor deposition

RFPECVD: Radio frequency plasma enhanced chemical vapor deposition

DCPECVD: Direct current plasma enhanced chemical vapor deposition

DPECVD: Diffusion plasma enhanced chemical vapor deposition

AAO: Anodic aluminum oxide

SS: Stainless-steel

VLS: Vapor-liquid-solid

Disclaimer

The details contained in this review article are for information purposes only. The authors, editors, and publisher cannot accept liability of any kind whatsoever for the accuracy of contents and data, any omissions or errors, or a claim of completeness.

Acknowledgement

The author AG would like to acknowledge the assistance provided by the funding agency, Department of Higher Education, Ministry of Human Resource Development, Government of India.

Competing interests

The authors declare that they have no competing interests.

Authors' contributions

AG carried out the literature survey on the patterned and vertical aligned CNTs and wrote the whole manuscript. CSS participated in its design and gave direction in writing the review. AKP gave an idea of such review and helped in tabulation of CNT arrays literature. He also helped in overall organization of the manuscript. All authors read and approved the final manuscript.

References

1. P. J. F. Harris, *Carbon Nanotubes and Related Structures: New Materials for the Twenty-first Century*, Cambridge, Cambridge University Press (1999).

2. M. S. Dresselhaus, G. Dresselhaus, and P. C. Eklund, *Science of Fullerenes and Carbon Nanotubes: Their Properties and Applications*, Academic Press (1996).
3. Z. K. Tang, L. Zhang, N. Wang, X. X. Zhang, G. H. Wen, G. D. Li, J. N. Wang, C. T. Chan, and P. Sheng, *Science* 292, 2462 (2001).
4. R. Ding, G. Lu, Z. Yan, and M. Wilson, *J. Nanosci. Nanotechnol.* 1, 7 (2001).
5. K. Mizuno, J. Ishii, H. Kishida, Y. Hayamizu, S. Yasuda, D. Futaba, M. Yumura, and K. Hata, *Proc. Natl. Acad. Sci. U. S. A.* 106, 6044 (2009).
6. Z.-P. Yang, L. Ci, J. A. Bur, S.-Y. Lin, and P. M. Ajayan, *Nano Lett.* 8, 446 (2008).
7. S. Shoji, H. Suzuki, R. P. Zaccaria, Z. Sekkat, and S. Kawata, *Phys. Rev. B* 77, 153407 (2008).
8. Y. Wang, K. Kempa, B. Kimball, J. Carlson, G. Benham, W. Li, T. Kempa, J. Rybczynski, A. Herczynski, and Z. Ren, *Appl. Phys. Lett.* 85, 2607 (2004).
9. X. Wang, J. Flicker, B. Lee, W. Ready, and Z. Zhang, *Nanotechnology* 20, 215704 (2009).
10. E. Lidorikis and A. C. Ferrari, *ACS Nano* 3, 1238 (2009).
11. K. Kempa, B. Kimball, J. Rybczynski, Z. P. Huang, P. F. Wu, D. Steeves, M. Sennett, M. Giersig, D. V. G. L. N. Rao, D. L. Carnahan, D. Z. Wang, J. Y. Lao, W. Z. Li, and Z. F. Ren, *Nano Lett.* 3, 13 (2003).
12. T. Xu, S. Yang, S. V. Nair, and H. E. Ruda, *Phys. Rev. B* 75, 125104 (2007).
13. R. E. Camacho, A. R. Morgan, M. C. Flores, T. A. McLeod, V. S. Kumsomboone, B. J. Mordecai, R. Bhattacharjea, W. Tong, B. K. Wagner, J. D. Flicker, S. P. Turano, and W. J. Ready, *JOM* 59, 39 (2007).
14. Z. Fan, H. Razavi, J. Do, A. Moriwaki, O. Ergen, Y.-L. Chueh, P. W. Leu, J. C. Ho, T. Takahashi, L. A. Reichertz, and others, *Nat. Mater.* 8, 648 (2009).
15. G. Chen, J. Wu, Q. Lu, H. R. Gutierrez, Q. Xiong, M. E. Pellen, J. S. Petko, D. H. Werner, and P. C. Eklund, *Nano Lett.* 8, 1341 (2008).
16. S. Yamashita, Y. Inoue, S. Maruyama, Y. Murakami, H. Yaguchi, M. Jablonski, and S. Y. Set, *Opt. Lett.* 29, 1581 (2004).
17. J. Koehne, H. Chen, J. Li, A. M. Cassell, Q. Ye, H. T. Ng, J. Han, and M. Meyyappan, *Nanotechnology* 14, 1239 (2003).
18. S.-H. Jeong, H.-Y. Hwang, K.-H. Lee, and Y. Jeong, *Appl. Phys. Lett.* 78, 2052 (2001).
19. L. Nilsson, O. Groening, C. Emmenegger, O. Kuettel, E. Schaller, L. Schlapbach, H. Kind, J.-M. Bonard, and K. Kern, *Appl. Phys. Lett.* 76, 2071 (2000).
20. K. Teo, M. Chhowalla, G. Amaratunga, W. Milne, G. Pirio, P. Legagneux, F. Wyczisk, D. Pribat, and D. Hasko, *Appl. Phys. Lett.* 80, 2011 (2002).
21. J.-M. Bonard, N. Weiss, H. Kind, T. Stöckli, L. Forró, K. Kern, and A. Chatelain, *Adv. Mater.* 13, 184 (2001).
22. Z. F. Ren, Z. P. Huang, D. Z. Wang, J. G. Wen, J. W. Xu, J. H. Wang, L. E. Calvet, J. Chen, J. F. Klemic, and M. A. Reed, *Appl. Phys. Lett.* 75, 1086 (1999).
23. K. Teo, M. Chhowalla, G. Amaratunga, W. Milne, P. Legagneux, G. Pirio, L. Gangloff, D. Pribat, V. Semet, V. T. Binh, and others, *J. Vac. Sci. Technol. B* 21, 693 (2003).
24. H. Ago, K. Murata, M. Yumura, J. Yotani, and S. Uemura, *Appl. Phys. Lett.* 82, 811 (2003).
25. J. D. Beard, J. Stringer, O. R. Ghita, and P. J. Smith, *ACS Appl. Mater. Interfaces* 5, 9785 (2013).
26. H. Kind, J.-M. Bonard, L. Forró, K. Kern, K. Hernadi, L.-O. Nilsson, and L. Schlapbach, *Langmuir* 16, 6877 (2000).
27. H. Kind, J.-M. Bonard, C. Emmenegger, L.-O. Nilsson, K. Hernadi, E. Maillard-Schaller, L. Schlapbach, L. Forró, and K. Kern, *Adv. Mater.* 11, 1285 (1999).
28. Y. Tu, Z. Huang, D. Wang, J. Wen, and Z. Ren, *Appl. Phys. Lett.* 80, 4018 (2002).
29. H. Shimoda, S. J. Oh, H. Z. Geng, R. J. Walker, X. B. Zhang, L. E. McNeil, and O. Zhou, *Adv. Mater.* 14, 899 (2002).
30. S. J. Tans, A. R. M. Verschueren, and C. Dekker, *Nature* 393, 49 (1998).

31. R. Martel, T. Schmidt, H. R. Shea, T. Hertel, and P. Avouris, *Appl. Phys. Lett.* 73, 2447 (1998).
32. M. S. Dresselhaus, G. Dresselhaus, and P. Avouris, Editors, *Carbon Nanotubes*, Berlin, Heidelberg, Springer Berlin Heidelberg (2001).
33. C. V. Nguyen, R. M. D. Stevens, J. Barber, J. Han, M. Meyyappan, M. I. Sanchez, C. Larson, and W. D. Hinsberg, *Appl. Phys. Lett.* 81, 901 (2002).
34. H. Zhang, G. Cao, Y. Yang, and Z. Gu, *J. Electrochem. Soc.* 155, K19 (2008).
35. C. Masarapu, V. Subramanian, H. Zhu, and B. Wei, *Adv. Funct. Mater.* 19, 1008 (2009).
36. J. Li, R. Stevens, L. Delzeit, H. T. Ng, A. Cassell, J. Han, and M. Meyyappan, *Appl. Phys. Lett.* 81, 910 (2002).
37. C. V. Nguyen, L. Delzeit, A. M. Cassell, J. Li, J. Han, and M. Meyyappan, *Nano Lett.* 2, 1079 (2002).
38. M. M. A. Rafique and J. Iqbal, *J. Encapsulation Adsorpt. Sci.* 1, 29 (2011).
39. S. Iijima, *J. Cryst. Growth* 50, 675 (1980).
40. H. W. Kroto, J. R. Heath, S. C. O'Brien, R. F. Curl, and R. E. Smalley, *Nature* 318, 162 (1985).
41. S. Iijima and others, *nature* 354, 56 (1991).
42. T. W. Ebbesen and P. M. Ajayan, *Nature* 358, 220 (1992).
43. S. Iijima and T. Ichihashi, *Nature* 363, 603 (1993).
44. D. S. Bethune, C. H. Klang, M. S. de Vries, G. Gorman, R. Savoy, J. Vazquez, and R. Beyers, *Nature* 363, 605 (1993).
45. C. Journet, W. K. Maser, P. Bernier, A. Loiseau, M. L. de la Chapelle, S. Lefrant, P. Deniard, R. Lee, and J. E. Fischer, *Nature* 388, 756 (1997).
46. M. Ushio, D. Fan, and M. Tanaka, *J. Phys. Appl. Phys.* 27, 561 (1994).
47. B. Ahmad, M. Ahmad, J. I. Akhter, and N. Ahmad, *Mater. Lett.* 59, 1585 (2005).
48. R. R. Ismagilov, P. V. Shvets, A. Y. Kharin, and A. N. Obratsov, *Crystallogr. Rep.* 56, 310 (2011).
49. T. Guo, P. Nikolaev, A. Thess, D. T. Colbert, and R. E. Smalley, *Chem. Phys. Lett.* 243, 49 (1995).
50. T. Guo, P. Nikolaev, A. G. Rinzler, D. Tomanek, D. T. Colbert, and R. E. Smalley, *J. Phys. Chem.* 99, 10694 (1995).
51. M. Ge and K. Sattler, *Phys. Chem. Fuller. Repr. Collect.* 1, 226 (1993).
52. Z. J. Kosakovskaja, L. Chernozatonskii, and E. Fedorov, *Jetp Lett.* 56, 26 (1992).
53. A. Thess, R. Lee, P. Nikolaev, H. Dai, P. Petit, J. Robert, C. Xu, Y. H. Lee, S. G. Kim, A. G. Rinzler, and others, *Sci.-AAAS-Wkly. Pap. Ed.* 273, 483 (1996).
54. P. L. Walker, J. F. Rakszawski, and G. R. Imperial, *J. Phys. Chem.* 63, 133 (1959).
55. M. José-Yacamán, M. Miki-Yoshida, L. Rendón, and J. G. Santiesteban, *Appl. Phys. Lett.* 62, 202 (1993).
56. null Li, null Xie, null Qian, null Chang, null Zou, null Zhou, null Zhao, and null Wang, *Science* 274, 1701 (1996).
57. Z. W. Pan, S. S. Xie, B. H. Chang, C. Y. Wang, L. Lu, W. Liu, W. Y. Zhou, W. Z. Li, and L. X. Qian, *Nature* 394, 631 (1998).
58. M. Terrones, N. Grobert, J. Olivares, J. P. Zhang, H. Terrones, K. Kordatos, W. K. Hsu, J. P. Hare, P. D. Townsend, K. Prassides, A. K. Cheetham, H. W. Kroto, and D. R. M. Walton, *Nature* 388, 52 (1997).
59. null Fan, null Chapline, null Franklin, null Tomblor, null Cassell, and null Dai, *Science* 283, 512 (1999).
60. V. B. Golovko, H. W. Li, B. Kleinsorge, S. Hofmann, J. Geng, M. Cantoro, Z. Yang, D. A. Jefferson, B. F. G. Johnson, W. T. S. Huck, and J. Robertson, *Nanotechnology* 16, 1636 (2005).
61. H. Zhu, C. Xu, D. Wu, B. Wei, R. Vajtai, and P. Ajayan, *Science* 296, 884 (2002).
62. Z. Ren, Z. Huang, J. Xu, J. Wang, P. Bush, M. Siegal, and P. Provencio, *Science* 282, 1105 (1998).
63. B. Kleinsorge, V. B. Golovko, S. Hofmann, J. Geng, D. Jefferson, J. Robertson, and B. F. G. Johnson, *Chem. Commun.* 1416 (2004).doi:10.1039/B401785D

64. B. O. Boskovic, V. B. Golovko, M. Cantoro, B. Kleinsorge, A. T. H. Chuang, C. Ducati, S. Hofmann, J. Robertson, and B. F. G. Johnson, *Carbon* 43, 2643 (2005).
65. M. Tanemura, K. Iwata, K. Takahashi, Y. Fujimoto, F. Okuyama, H. Sugie, and V. Filip, *J. Appl. Phys.* 90, 1529 (2001).
66. M. Meyyappan, L. Delzeit, A. Cassell, and D. Hash, *Plasma Sources Sci. Technol.* 12, 205 (2003).
67. H. Sato and K. Hata, *New Diam. Front. Carbon Technol.* 16, 163 (2006).
68. A. V. Melechko, V. I. Merkulov, T. E. McKnight, M. A. Guillorn, K. L. Klein, D. H. Lowndes, and M. L. Simpson, *J. Appl. Phys.* 97, 41301 (2005).
69. M. A. Azam, K. Isomura, A. Fujiwara, and T. Shimoda, *Phys. Status Solidi A* 209, 2260 (2012).
70. A. Suriani, A. Dalila, A. Mohamed, M. Mamat, M. Salina, M. Rosmi, J. Rosly, R. M. Nor, and M. Rusop, *Mater. Lett.* 101, 61 (2013).
71. R. Reit, J. Nguyen, and W. J. Ready, *Electrochimica Acta* 91, 96 (2013).
72. W. Cho, M. Schulz, and V. Shanov, *Carbon* 72, 264 (2014).
73. Y. Li, J. Kang, J.-B. Choi, J.-D. Nam, and J. Suhr, *Nanotechnology* 26, 245701 (2015).
74. M. W. Lee, M. A. S. M. Haniff, A. S. Teh, D. C. S. Bien, and S. K. Chen, *J. Exp. Nanosci.* 10, 1232 (2015).
75. H. K. Jung and H. W. Lee, *J. Nanomater.* 2014, e270989 (2014).
76. J. Li, C. Papadopoulos, and J. Xu, *Nature* 402, 253 (1999).
77. J. Li, C. Papadopoulos, J. M. Xu, and M. Moskovits, *Appl. Phys. Lett.* 75, 367 (1999).
78. M.-W. Li, Z. Hu, X.-Z. Wang, Q. Wu, and Y. Chen, *J. Mater. Sci. Lett.* 22, 1223 (2003).
79. X. Xu and G. R. Brandes, *Appl. Phys. Lett.* 74, 2549 (1999).
80. Y. Y. Wei, G. Eres, V. I. Merkulov, and D. H. Lowndes, *Appl. Phys. Lett.* 78, 1394 (2001).
81. M. A. Signore, A. Rizzo, R. Rossi, E. Piscopiello, T. Di Luccio, L. Capodici, T. Dikonimos, and R. Giorgi, *Diam. Relat. Mater.* 17, 1936 (2008).
82. W. Z. Li, D. Z. Wang, S. X. Yang, J. G. Wen, and Z. F. Ren, *Chem. Phys. Lett.* 335, 141 (2001).
83. E. T. Thostenson, W. Z. Li, D. Z. Wang, Z. F. Ren, and T. W. Chou, *J. Appl. Phys.* 91, 6034 (2002).
84. C. Masarapu and B. Wei, *Langmuir* 23, 9046 (2007).
85. Y. Homma, *Catalysts* 4, 38 (2014).
86. R. T. K. Baker, M. A. Barber, P. S. Harris, F. S. Feates, and R. J. Waite, *J. Catal.* 26, 51 (1972).
87. A. Oberlin, M. Endo, and T. Koyama, *J. Cryst. Growth* 32, 335 (1976).
88. S. Amelinckx, X. B. Zhang, D. Bernaerts, X. F. Zhang, V. Ivanov, and J. B. Nagy, *Science* 265, 635 (1994).
89. S. Helveg, C. López-Cartes, J. Sehested, P. L. Hansen, B. S. Clausen, J. R. Rostrup-Nielsen, F. Abild-Pedersen, and J. K. Nørskov, *Nature* 427, 426 (2004).
90. F. Ding, K. Bolton, and A. Rosen, *J. Phys. Chem. B* 108, 17369 (2004).
91. J. B. Nagy, G. Bister, A. Fonseca, D. Méhn, Z. Kónya, I. Kiricsi, Z. E. Horváth, and L. P. Biró, *J. Nanosci. Nanotechnol.* 4, 326 (2004).
92. Atomic-Resolution Imaging of the Nucleation Points of Single-Walled Carbon Nanotubes - Zhu - 2005 - Small - Wiley Online Library at <<http://onlinelibrary.wiley.com/doi/10.1002/sml.200500200/abstract>>
93. M. Audier and M. Coulon, *Carbon* 23, 317 (1985).
94. M. Endo, K. Takeuchi, K. Kobori, K. Takahashi, H. W. Kroto, and A. Sarkar, *Carbon* 33, 873 (1995).
95. T. W. Ebbesen, *Carbon nanotubes: preparation and properties*, CRC press (1996).
96. M. Yudasaka, R. Kikuchi, Y. Ohki, E. Ota, and S. Yoshimura, *Appl. Phys. Lett.* 70, 1817 (1997).
97. J.-C. Charlier, A. De Vita, X. Blase, and R. Car, *Science* 275, 647 (1997).
98. J.-C. Charlier and S. Iijima, Growth mechanisms of carbon nanotubes, in *Carbon Nanotubes*, Springer (2001), pp. 55–81.
99. R. T. K. Baker, *Carbon* 27, 315 (1989).

100. R. T. K. Baker and R. J. Waite, *J. Catal.* 37, 101 (1975).
101. R. Baker, P. Harris, P. Walker Jr, and P. Thrower, *Vol 14 Marcel Dekker N. Y.* 83 (1978).
102. R. Baker, *J. Catal.* 64, 464 (1980).
103. W. Y. Lee, T. X. Liao, Z. Y. Juang, and C. H. Tsai, *Diam. Relat. Mater.* 13, 1232 (2004).
104. T. X. Li, H. G. Zhang, F. J. Wang, Z. Chen, and K. Saito, *Proc. Combust. Inst.* 31, 1849 (2007).
105. T. X. Li, K. Kuwana, K. Saito, H. Zhang, and Z. Chen, *Proc. Combust. Inst.* 32, 1855 (2009).
106. Y. Yun, V. Shanov, Y. Tu, S. Subramaniam, and M. J. Schulz, *J. Phys. Chem. B* 110, 23920 (2006).
107. Y. J. Jung, B. Wei, R. Vajtai, P. M. Ajayan, Y. Homma, K. Prabhakaran, and T. Ogino, *Nano Lett.* 3, 561 (2003).
108. Z. J. Zhang, B. Q. Wei, G. Ramanath, and P. M. Ajayan, *Appl. Phys. Lett.* 77, 3764 (2000).
109. L. Delzeit, C. V. Nguyen, B. Chen, R. Stevens, A. Cassell, J. Han, and M. Meyyappan, *J. Phys. Chem. B* 106, 5629 (2002).
110. C. Zhang, S. Pisana, C. T. Wirth, A. Parvez, C. Ducati, S. Hofmann, and J. Robertson, *Diam. Relat. Mater.* 17, 1447 (2008).
111. H. Liu, Y. Zhang, D. Arato, R. Li, P. Mérel, and X. Sun, *Surf. Coat. Technol.* 202, 4114 (2008).
112. D. B. Thakur, R. M. Tiggelaar, J. G. E. Gardeniers, L. Lefferts, and K. Seshan, *Surf. Coat. Technol.* 203, 3435 (2009).
113. W.-P. Wang, H.-C. Wen, S.-R. Jian, J.-Y. Juang, Y.-S. Lai, C.-H. Tsai, W.-F. Wu, K.-T. Chen, and C.-P. Chou, *Appl. Surf. Sci.* 253, 9248 (2007).
114. N. Yamamoto, A. John Hart, E. J. Garcia, S. S. Wicks, H. M. Duong, A. H. Slocum, and B. L. Wardle, *Carbon* 47, 551 (2009).
115. G. W. Ho, A. T. S. Wee, J. Lin, and W. C. Tjiu, *Thin Solid Films* 388, 73 (2001).
116. S. S. Xie, B. H. Chang, W. Z. Li, Z. W. Pan, L. F. Sun, J. M. Mao, X. H. Chen, L. X. Qian, and W. Y. Zhou, *Adv. Mater.* 11, 1135 (1999).
117. Y. Murakami, S. Yamakita, T. Okubo, and S. Maruyama, *Chem. Phys. Lett.* 375, 393 (2003).
118. R. Xiang, G. H. Luo, W. Z. Qian, Y. Wang, F. Wei, and Q. Li, *Chem. Vap. Depos.* 13, 533 (2007).
119. Q. Zhang, J.-Q. Huang, M.-Q. Zhao, W.-Z. Qian, Y. Wang, and F. Wei, *Carbon* 46, 1152 (2008).
120. Q. Zhang, M.-Q. Zhao, J.-Q. Huang, Y. Liu, Y. Wang, W.-Z. Qian, and F. Wei, *Carbon* 47, 2600 (2009).
121. S. Hofmann, M. Cantoro, B. Kleinsorge, C. Casiraghi, A. Parvez, J. Robertson, and C. Ducati, *J. Appl. Phys.* 98, 34308 (2005).
122. Y. Wang, J. Rybczynski, D. Z. Wang, K. Kempa, Z. F. Ren, W. Z. Li, and B. Kimball, *Appl. Phys. Lett.* 85, 4741 (2004).
123. A. V. Melechko, T. E. McKnight, D. K. Hensley, M. A. Guillorn, A. Y. Borisevich, V. I. Merkulov, D. H. Lowndes, and M. L. Simpson, *Nanotechnology* 14, 1029 (2003).
124. M. Chhowalla, K. B. K. Teo, C. Ducati, N. L. Rupesinghe, G. a. J. Amaratunga, A. C. Ferrari, D. Roy, J. Robertson, and W. I. Milne, *J. Appl. Phys.* 90, 5308 (2001).
125. M. Seita, *MSc thesis, Department of Electrical Engineering, (research done at Massachusetts Institute of Technology), (2007).*
126. M. Monthieux and V. L. Kuznetsov, *Carbon* 44, 1621 (2006).
127. W. Bollmann and J. Spreadborough, *Nature* 186, 29 (1960).
128. T. Koyama and M. Endo, *Jpn. Pat. No* 58 (1982).
129. M. Endo, *Chemtech* 18, 568 (1988).
130. J. W. Mintmire, B. I. Dunlap, and C. T. White, *Phys. Rev. Lett.* 68, 631 (1992).
131. N. Hamada, S. Sawada, and A. Oshiyama, *Phys. Rev. Lett.* 68, 1579 (1992).
132. R. Saito, M. Fujita, G. Dresselhaus, and M. S. Dresselhaus, *Phys. Rev. B* 46, 1804 (1992).
133. G. Overney, W. Zhong, and D. Tománek, *Z. Für Phys. At. Mol. Clust.* 27, 93 (1993).
134. A. Rinzler, J. Hafner, P. Nikolaev, L. Lou, S. Kim, D. Tomanek, P. Nordlander, D. Colbert, and R. Smalley, *Sci.-N. Y. THEN Wash.-* 1550 (1995).

135. S. J. Tans, M. H. Devoret, H. Dai, A. Thess, R. E. Smalley, L. J. Georliga, and C. Dekker, *Nat.* 3866624 474-477 1997 (1997).at <<http://repository.tudelft.nl/view/ir/uuid:4e58e2bc-5f69-4dbe-9942-aabcc9eaad35/>>
136. M. Bockrath, D. H. Cobden, P. L. McEuen, N. G. Chopra, A. Zettl, A. Thess, and R. E. Smalley, *Science* 275, 1922 (1997).
137. A. D. K. Jones and T. Bekkedahl, *Nature* 386, 377 (1997).
138. H. Cheng, F. Li, X. Sun, S. Brown, M. Pimenta, A. Marucci, G. Dresselhaus, and M. Dresselhaus, *Chem. Phys. Lett.* 289, 602 (1998).
139. B. W. Smith, M. Monthieux, and D. E. Luzzi, *Nature* 396, 323 (1998).
140. S. Berber, Y.-K. Kwon, and D. Tománek, *Phys. Rev. Lett.* 84, 4613 (2000).
141. B. Vigolo, A. Penicaud, C. Coulon, C. Sauder, R. Pailier, C. Journet, P. Bernier, and P. Poulin, *Science* 290, 1331 (2000).
142. T. W. Tomblor, C. Zhou, L. Alexseyev, J. Kong, H. Dai, L. Liu, C. S. Jayanthi, M. Tang, and S.-Y. Wu, *Nature* 405, 769 (2000).
143. P. G. Collins, M. S. Arnold, and P. Avouris, *science* 292, 706 (2001).
144. M. Kociak, A. Y. Kasumov, S. Guéron, B. Reulet, I. I. Khodos, Y. B. Gorbatov, V. T. Volkov, L. Vaccarini, and H. Bouchiat, *Phys. Rev. Lett.* 86, 2416 (2001).
145. J. Minkel, *Physics* 9, 4 (2002).
146. K. Hata, D. N. Futaba, K. Mizuno, T. Namai, M. Yumura, and S. Iijima, *Science* 306, 1362 (2004).
147. L. X. Zheng, M. J. O'Connell, S. K. Doorn, X. Z. Liao, Y. H. Zhao, E. A. Akhadov, M. A. Hoffbauer, B. J. Roop, Q. X. Jia, R. C. Dye, D. E. Peterson, S. M. Huang, J. Liu, and Y. T. Zhu, *Nat. Mater.* 3, 673 (2004).
148. K. S. Novoselov, A. K. Geim, S. Morozov, D. Jiang, Y. Zhang, S. Dubonos, I. and Grigorieva, and A. Firsov, *science* 306, 666 (2004).
149. A. R. Harutyunyan, G. Chen, T. M. Paronyan, E. M. Pigos, O. A. Kuznetsov, K. Hewaparakrama, S. M. Kim, D. Zakharov, E. A. Stach, and G. U. Sumanasekera, *Science* 326, 116 (2009).
150. New virus-built battery could power cars, electronic devicesat <<http://news.mit.edu/2009/virus-battery-0402>>
151. CNano Technology Commissions World's Largest Carbon Nanotube Manufacturing Plant With a Capacity of 500 Tons per Yearat <<http://www.marketwired.com/press-release/cnano-technology-commissions-worlds-largest-carbon-nanotube-manufacturing-plant-with-1220714.htm>>
152. Q. Wen, R. Zhang, W. Qian, Y. Wang, P. Tan, J. Nie, and F. Wei, *Chem. Mater.* 22, 1294 (2010).
153. S. A. on J. 26 and 2012 at 7:05 Am, IBM creates 9nm carbon nanotube transistor that outperforms siliconat <<http://www.extremetech.com/computing/115657-ibm-creates-9nm-carbon-nanotube-transistor-outperforms-silicon>>
154. M. M. Shulaker, G. Hills, N. Patil, H. Wei, H.-Y. Chen, H.-S. P. Wong, and S. Mitra, *Nature* 501, 526 (2013).
155. Y. C. Choi, Y. M. Shin, Y. H. Lee, B. S. Lee, G.-S. Park, W. B. Choi, N. S. Lee, and J. M. Kim, *Appl. Phys. Lett.* 76, 2367 (2000).
156. Y. H. Wang, J. Lin, C. H. A. Huan, and G. S. Chen, *Appl. Phys. Lett.* 79, 680 (2001).
157. C. J. Lee and J. Park, *Carbon* 39, 1891 (2001).
158. S. Chakrabarti, T. Nagasaka, Y. Yoshikawa, L. Pan, and Y. Nakayama, *Jpn. J. Appl. Phys.* 45, L720 (2006).
159. M. Hiramatsu, T. Deguchi, H. Nagao, and M. Hori, *Diam. Relat. Mater.* 16, 1126 (2007).
160. R. Xiang, Z. Zhang, K. Ogura, J. Okawa, E. Einarsson, Y. Miyauchi, J. Shiomi, and S. Maruyama, *Jpn. J. Appl. Phys.* 47, 1971 (2008).
161. L. Gao, A. Peng, Z. Y. Wang, H. Zhang, Z. Shi, Z. Gu, G. Cao, and B. Ding, *Solid State Commun.* 146, 380 (2008).

162. X. Liu, K. H. R. Baronian, and A. J. Downard, *Carbon* 47, 500 (2009).
163. H. Sugime, S. Noda, S. Maruyama, and Y. Yamaguchi, *Carbon* 47, 234 (2009).
164. B. Kim, H. Chung, K. S. Chu, H. G. Yoon, C. J. Lee, and W. Kim, *Synth. Met.* 160, 584 (2010).
165. B. Kim, H. Chung, B. K. Min, H. Kim, and W. Kim, *Bull Korean Chem Soc* 31, 3697 (2010).
166. R. Löffler, M. Häffner, G. Visanescu, H. Weigand, X. Wang, D. Zhang, M. Fleischer, A. J. Meixner, J. Fortágh, and D. P. Kern, *Carbon* 49, 4197 (2011).
167. P. Dong, C. L. Pint, M. Hainey, F. Mirri, Y. Zhan, J. Zhang, M. Pasquali, R. H. Hauge, R. Verduzco, M. Jiang, H. Lin, and J. Lou, *ACS Appl. Mater. Interfaces* 3, 3157 (2011).
168. S. P. Patole, H.-I. Kim, J.-H. Jung, A. S. Patole, H.-J. Kim, I.-T. Han, V. N. Bhoraskar, and J.-B. Yoo, *Carbon* 49, 3522 (2011).
169. Y. H. Gwon, J. K. Ha, K. K. Cho, and H. S. Kim, *Nanoscale Res. Lett.* 7, 1 (2012).
170. K. Y. JEONG, H. K. JUNG, and H. W. LEE, *Trans. Nonferrous Met. Soc. China* 22, Supplement 3, s712 (2012).
171. S. Neupane, M. Lastres, M. Chiarella, W. Li, Q. Su, and G. Du, *Carbon* 50, 2641 (2012).
172. T. Thurakitserree, C. Kramberger, P. Zhao, S. Aikawa, S. Harish, S. Chiashi, E. Einarsson, and S. Maruyama, *Carbon* 50, 2635 (2012).
173. J. Choi, Y. Eun, S. Pyo, J. Sim, and J. Kim, *Microelectron. Eng.* 98, 405 (2012).
174. S. Kumar, I. Levchenko, K. K. Ostrikov, and J. A. McLaughlin, *Carbon* 50, 325 (2012).
175. K. B. K. Teo, M. Chhowalla, G. a. J. Amaratunga, W. I. Milne, D. G. Hasko, G. Pirio, P. Legagneux, F. Wycisk, and D. Pribat, *Appl. Phys. Lett.* 79, 1534 (2001).

List of Table:

Table 1. Table shows the yearly incidents and corresponding publications in the development of CNTs structures, properties and applications.

Table 2. Table shows the concise comparison of different methods to grow CNTs (source: Seita [125] with data compiled from many sources).

Table 3. Table comprises the comprehensive summary of the process parameters and their effects on the growth of Vertical Aligned CNTs by Catalytic CVD method.

Table 1. Table shows the yearly incidents and corresponding publications in the development of CNTs structures, properties and applications.

Year	Key events	Group	Ref.
1889	Formation of carbon filaments by decomposition of methane	Hughes and Chambers	[126]
1890	Formation of carbon filaments on red-hot porcelain	Schutzenberger and Schutzenberger	[126]
1952	First TEM images of hollow graphitic carbon nanofilaments or fibres (50 nanometers in diameter)	Radushkevich and Lukyanovich	[126]
1960	Friction properties of carbon due to rolling sheets of graphene in Nature. Electron Microscope picture clearly shows MWCNT.	Bollmann and Spreadborough	[127]
1976	First TEM image of a thin, hollow carbon nanofilament (probably a MWCNT) and CVD growth of nanometer-scale carbon fibers and also the discovery of carbon nanofibers, including that some were shaped as hollow tubes.	Oberlin et al.	[87]
1982	The continuous or floating-catalyst process was patented by Japanese researcher Morinobu Endo	Koyama and Endo	[128, 129]
1991	Discovery of multi-wall carbon nanotubes (by arc discharge, structural investigation by HRTEM)	Iijima et al.	[41]
1992	First theoretical predictions of the electronic properties of SWCNTs or Conductivity of carbon nanotubes	Mintmire et. al., Hamada et. al. and Saito et. al.	[130–132]
1993	Structural rigidity of carbon nanotubes	Overney et. al	[133]

1993	First reports on the formation of SWCNTs during arc discharge synthesis using transition metal catalysts.	Iijima et al. and Bethune et al.	[43, 44]
1995	Nanotubes as field emitters	Rinzler et. al.	[134]
1996	Growth of aligned MWCNTs from Fe particles embedded in mesoporous silica (50µm long and spacing between the tubes of about 100 nm)	Li et al.	[56]
1996	Ropes of single-wall nanotubes	Thess et. al.	[53]
1997	Optimized fabrication of SWCNTs by arc discharge (70-90% selectivity)	Journet et al.	[45]
1997	Quantum conductance of carbon nanotubes and First CNT single-electron transistors (operating at low temperature) are demonstrated	Tans et al. and Bockrath et al.	[135, 136]
1997	Hydrogen storage in nanotubes	Dillon et al.	[137]
1998	Chemical Vapor Deposition synthesis of aligned nanotube films	Ren et al.	[62]
1998	First large-scale synthesis of SWCNTs by CCVD	Cheng et al.	[138]
1998	Synthesis of nanotube peapods	Smith et al.	[139]
1999	Patterned growth of aligned carbon nanotubes on Silicon wafers	Fan et al.	[59]
2000	Thermal conductivity of nanotubes	Berber et al.	[140]
2000	Macroscopically aligned nanotubes	Vigolo et al.	[141]
2000	First demonstration to show that bending CNTs changes their resistance	Tombler et al.	[142]
2001	First report on a technique for separating semiconducting and metallic nanotubes and Integration of carbon nanotubes for logic circuits	Collins et al.	[143]
2001	Intrinsic superconductivity of carbon nanotubes	Kociak et al.	[144]
2002	MWCNTs demonstrated to be fastest known oscillators (> 50 GHz)		[145]
2004	Enhanced growth (super-growth) of SWCNTs in the presence of H ₂ O	Hata et al.	[146]
2004	Nature published a photo of an individual 4 cm long single-wall nanotube (SWCNT)	Zheng et al.	[147]
2004	Report on Graphene	Novoselov et al.	[148]
2009	Improved selectivity to metallic SWCNT by very careful preconditioning and refining of the catalyst	Harutyunyan et al.	[149]
2009	Nanotubes incorporated in virus battery		[150]
2009	World's biggest MWCNT production plant having capacity of 500 tones/year is inaugurated	CNano Technology	[151]
2010	Growth of 20 cm long DWCNTs/TWCNTs	Wen et al.	[152]
2012	IBM creates 9nm CNT transistor that outperforms silicon	IBM	[153]
2013	Completely CNTs based transistors used in computer named Cedric	Shulaker et al.	[154]

Table 2. Table shows the concise comparison of different methods to grow CNTs

Method / Feature	Arc-discharge	Laser Ablation	CVD	
			Thermal CVD	PECVD
Type of process	Physical	Physical	Chemical	
Need of energy	High	High	Moderate	
Raw materials finding	Difficult	Difficult	Easily available	
Chamber design	Difficult	Difficult	Designed as large scale process	
Process control	Difficult	Difficult	Easy (automated)	
Operating temperature ($^{\circ}\text{C}$)*	~4000	Room temp to 1000	500-1200	100-800
Production rate	Low	Low	High	
CNT growth rate/ $\mu\text{m s}^{-1}$ *	Up to 10^7	~0.1	0.1-10	0.01-1
Product cleanliness*	Low	Low	Medium to High	Medium
Post treatments	Require refining	Require refining	No need of extensive refining	
Nature of Process (continuous or batch)	Batch type	Batch type	Continuous type	
CNT length/ μm *	~1	~1	$0.1-10^5$	0.1-10
Yield of process	Moderate (70%)	High (80%-85%)	High (95%-99%)	
Per unit cost	High	High	Low	

(Source: *Data were adapted from [125], M. Seita, MSc thesis, Department of Electrical Engineering, (research done at Massachusetts Institute of Technology), (2007).

Table 3. Table comprises the comprehensive summary of the process parameters and their effects on the growth of Vertical Aligned CNTs by Catalytic CVD method.

Catalyst, Catalyst support and Substrate	Reaction condition				Type of CNT (Dimension)	Remarks	Ref	
	Flow rate of gases (sccm)		Temp ($^{\circ}$ C)	Pressure (kPa)				Time (min)
	Carbon source	Carrier Gas						
Catalyst: Ni Catalyst support: Substrate: Si	CH ₄	H ₂	700	1.33	5 min	VAMWCNT with diameter of 10-35 nm and thickness ~40 μ m. Fastest growth rate was 85 μ m/min	Microwave power during CNT growth 400 W RF power density adjusted for better CNT density and growth rate.	[155]
Catalyst: Fe Catalyst support: SiO ₂ Substrate: Si	C ₂ H ₂ (15 sccm)	H ₂ (60 sccm)	700	0.16	5-20 min	H ₂ plasma (60 sccm) treatment grown VAMWCNT with diameter of 10-35 nm and thickness of 5-20 μ m Growth rate 1 μ m/min	RF is 13.56 MHz with power at 100 W	[156]
Catalyst: Co Catalyst support: SiO ₂ Substrate: Si	C ₂ H ₂ (40 sccm)	NH ₃ (200 sccm)	950	-	10 min	Bamboo shaped VAMWCNT with diameter of 80-120 nm with thickness of 20 μ m	30 min NH ₃ flowed and Argon during raising-lowering temperature	[157]
Catalyst: Fe Catalyst support: Al ₂ O ₃ Substrate: Si/SiO ₂	C ₂ H ₄ (15 sccm)	He/H ₂ (105/15 sccm)	750	-	30 min	VADWCNT with thickness of 7 nm	Water vapor	[158]
Catalyst: Co/Ti Catalyst support: Substrate: Si	CH ₄ (50 sccm)	H ₂ (70 sccm)	700	0.93	5 min	VASWCNT with diameter of 1-2 nm and thickness of 60-70 μ m	2.45 GHz of microwave plasma power at 900 W	[159]
Catalyst: Co Catalyst support: Mo Substrate: Quartz	C ₂ H ₅ OH	Ar/H ₂ (300/300 sccm)	750-850	0.3-2.0	10 min	VASWCNT with thickness of 25 μ m	No flow of feedstock gas. It introduced after reaching desire pressure in CCVD	[160]

Catalyst: Fe Catalyst support: SiO ₂ Substrate: Si	C ₂ H ₄	Ar/H ₂ (300/40 sccm)	800	-	120 min	VAMWCNT with diameter of 12-16 nm and thickness of 150 μm	-	[161]
Catalyst: Fe Catalyst support: Al Substrate: PPF; Pyrolyzed photoresist film	C ₂ H ₄ (400 sccm)	Ar/H ₂ (300/200 sccm)	750	-	20 min	VAMWCNT diameter of 10-20 nm and thickness of 1 mm density of VAMWCNT bundle is more than 108 CNT per cm ²	Water vapor (50-100 sccm), during heating ratio of Ar/H ₂ (1200/800 sccm) is used	[162]
Catalyst: Co, Mo Substrate: Si	C ₂ H ₅ OH (4.9, 25, 140 sccm)	Ar/H ₂ (20 sccm)	747, 847, 947	1.3, 4, 12	10 min	VASWCNT diameter of 2-3 nm depends on	C ₂ H ₅ OH pressure and temperature in the chamber affects Catalyst efficiency	[163]
Catalyst: Fe Catalyst support: Al ₂ O ₃ Substrate: Stainless steel	C ₂ H ₄ (50 sccm)	Ar/H ₂ (125/100 sccm)	800	-	20 min	VAMWCNT having diameter of 10 nm and thickness of 400 μm Growth rate 20 μm/min and without H ₂ O vapor the thickness is 50 μm	Water vapor (0.75 sccm)	[164]
Catalyst: Fe Catalyst support: Al ₂ O ₃ Substrate: Ta	C ₂ H ₄ (50 sccm)	Ar/H ₂ (125/100 sccm)	800	-	5 min	VADWCNT having mean diameter 7 nm Growth rate 160 μm/min and thickness 800 μm	Water vapor (0.75 sccm)	[165]
Catalyst: Ni Catalyst support: SiO ₂ Substrate: Si	C ₂ H ₂	NH ₃	600	0.43	10 min	VACNT growth depend on the CCVD process parameters	Plasma power at 10 W, 15 kHz AC NH ₃ /C ₂ H ₂ ratio of 5:1	[166]
Catalyst: Fe Catalyst support: Al ₂ O ₃ Substrate: Si	C ₂ H ₂	H ₂	750	0.187	3-5 min	VASWCNT with thickness of 50-60 μm	Water vapor	[167]
Catalyst: FeCl ₃ Barrier layer: Al Substrate: Stainless steel	C ₂ H ₂ (200 sccm)	Ar (500 sccm)	810	0.32	10 min	VAMWCNT having 3-8 nm diameter and 600 μm thickness	Water vapor	[168]
Catalyst: Ni Catalyst support: Au Substrate: Ti	C ₂ H ₂	NH ₃	900	-	10 min	VAMWCNT having diameter 80-120 nm and thickness 10 μm	-	[169]
Catalyst: Ni Catalyst support: SiO ₂ Substrate: Si	C ₂ H ₂	NH ₃	750	0.6	5 min	Uniformly VAMWCNT of diameter 50 nm obtained at 100 W	Combination of plasma and thermal CCVD Plasma power 80 W	[170]
Catalyst: Ni Catalyst support: Cr Substrate: Cu	C ₂ H ₂ (30 sccm)	NH ₃ (100 sccm)	520	1.06	10 min	VACNTs of length between 1-2 μm and diameter in the range of 80-100 nm have grown. The density and location of CNTs determined by the diameter of spheres	The power of the DC plasma was 70 W. Ni catalyst nanodots diameter 0.5, 1.0, and 1.8 μm patterned by nanosphere lithography.	[171]

Catalyst: Co Catalyst support: Mo Substrate: Quartz	CH ₃ CN mixed C ₂ H ₅ OH	Ar/H ₂ (300/300 sccm)	800	1.7	3 min	VASWCNT with diameter of 0.7-2.1 nm and thickness of 25-30 μm	Ar/H ₂ pressure was 40 kPa Feedstock gas of 40 μL fed after reaching growth temperature.	[172]
Catalyst: Fe Catalyst support: SiO ₂ Substrate: Si	C ₂ H ₂ (50 sccm)	NH ₃ (100 sccm)	750	0.3	30 min	VACNT with thickness of 5 μm		[173]
Catalyst: Si (100) Substrate: Si	CH ₄	N ₂	850	2.67	3-5 min	VAMWCNT with diameter of 15-50 nm Growth rate 50 μm/min Array density 1000 nanotubes/ μm ²	Microwave plasma power at 700 W N ₂ at 0.93 kPa with 200 W plasma power during heating.	[174]
Catalyst: Co Catalyst support: Al ₂ O ₃ Substrate: stainless steel	C ₂ H ₅ OH (100-130 sccm)	Ar/H ₂	700	3	10 min	VASWCNT with 50 μm thickness.	-	[69]
Catalyst: C ₁₀ H ₁₀ Fe mixed with waste chicken fat oil Catalyst support: SiO ₂ Substrate: Si	Chicken fat	Ar	750	-	60 min	VAMWCNT with diameter of 18-78 nm and thickness of 20-25 μm Purity of 88.2%	Reaction chamber temperature 470°C Molecules of Chicken oil decomposed into hydrocarbon and catalytically decomposing on the Fe surface.	[70]
Catalyst: Fe Catalyst support: Ni/Ti/Al Substrate: Al	C ₂ H ₂ (700 sccm)	H ₂ (100 sccm)	700	-	5-25 min	VAMWCNT with diameter of 20 nm and thickness 5.3 μm at 5 min to 6.8 μm at 25 min	Low pressure Catalytic CVD	[71]
Catalyst: Fe-Gd Catalyst support: Al ₂ O ₃ Substrate: Si/SiO ₂	C ₂ H ₄ (140 mmHg)	Ar:H ₂ (560:60 mmHg)	780-820	-	790 min	21.7 mm long VAMWCNT array grown with 27.47 μm/min growth rate at 780 C. The growth rate at 780, 800, and 820°C was 27.22, 40.5, 58.64 μm/min respectively.	Water vapor was 600 ppm. The ID/IG peaks at bottom, middle and top portions of the tubes were 0.765, 0.86 and 0.90 respectively.	[72]
Catalyst: Fe Catalyst support: Al Substrate: Si/SiO ₂	C ₂ H ₄ (35 sccm)	Ar:H ₂ (200:55 sccm)	850	-	120 min	The outer and inner diameters of VAMWCNTs are 23 ± 2 nm and 7 ± 1 nm respectively. The average number of graphitic layers of the nanotube is ~22. The density of the VACNT is 0.045 g cm ⁻³	The average ID/IG ratio from the Raman spectrum analysis is 1.23 with 2.2% standard deviation.	[73]

List of Figures:

Figure 1: Experimental set up to produce CNTs by Laser ablation method. Reproduced with permission from [38], M. M. A. Rafique and J. Iqbal, *J. Encapsulation Adsorpt. Sci.* 1, 29 (2011). Copyright@ Scientific Research Publishing.

Figure 2. (a–d) SEM images of vertically aligned carbon nanotube forests localized at catalyst sites deposited by inkjet printing, using (a) 1, (b) 8, (c) 27, (d) 64 drops/site. The 27- and 64-drop sites show less uniform growth than those grown with 1 and 8 drops/site, with vacancies within the nanotube forests. The forests in (d) show vertically aligned growth concentrated in concentric rings within the deposition site. These rings may arise due to the “coffee-ring” effect that produces non uniform distribution of catalyst particles within the printed region. (e) Magnified view of nanotube forest sidewall, from a forest grown using 64 drops/site of catalyst suspension, showing strong vertical alignment within the forest capped by a disordered “tangle” at the forest top. (f) Increased magnification image of forest sidewall, in this case from a forest grown using 27 drops/site, showing CNT alignment. (g) Example of a nanotube forest grown using catalyst patterned by electron beam lithography for comparative purposes. Reprinted with permission from ref. [25], J. D. Beard, J. Stringer, O. R. Ghita, and P. J. Smith, *ACS Appl. Mater. Interfaces* 5, 9785 (2013). Copyright@ American Chemical Society.

Figure 3. (A) A series of SEM micrographs from different viewing angles showing growth of carbon nanotube obelisks on an array of submicron nickel dots. (a) An inclined view of a repeated array pattern. (b) A top (normal) view of a repeated array pattern. (c) An inclined view of one array pattern. (d) A top (normal) view of one array pattern. The initial Ni dots (and subsequently the grown carbon structures) are spaced either 2 μm apart (left) or 1 μm apart (right). (e) A magnified view along the edge of one pattern. A sharp, tapered tip is evident. (f) An inclined view of carbon obelisks grown on nickel dots separated by 5 μm . Reprinted with permission from ref. [22] F. Ren, Z.P. Huang, D.Z. Wang, J.G. Wen, J.W. Xu, J.H. Wang, L.E. Calvet, J. Chen, J.F. Klemic, M.A. Reed, *Appl. Phys. Lett.* 75, 1086 (1999). Copyright@ American Institute of Physics. (B) (a) Bunches of nanotubes (~100 nm in diameter) are deposited on 1 μm nickel dots because the nickel catalyst film breaks up into multiple nanoparticles. (b) Single nanotubes are deposited when the nickel dot size is reduced to 100 nm as only a single nickel nanoparticle is formed from the dot. (c) Demonstration of high yield, uniform, and selective growth of nanotubes at different densities. Reprinted with permission from ref. [175], B.K. Teo, M. Chhowalla, G.A.I. Amaratunga, W.I. Milne, D.G. Hasko, G. Pirio, P. Legagneux, F. Wyczisk, D. Pribat, *Appl. Phys. Lett.* 79, 1534 (2001). Copyright@ American Institute of Physics.

Figure 4: SEM images of Ni films with varying thicknesses deposited using magnetron sputtering on 50 nm of SiO_2 after annealing at 750 $^\circ\text{C}$ in 20 Torr of H_2 for 15 minutes. Reprinted with permission from [124], M. Chhowalla, K. B. K. Teo, C. Ducati, N. L. Rupesinghe, G. a. J. Amaratunga, A. C. Ferrari, D. Roy, J. Robertson, and W. I. Milne, *J. Appl. Phys.* 90, 5308 (2001). Copyright@ American Institute of Physics.

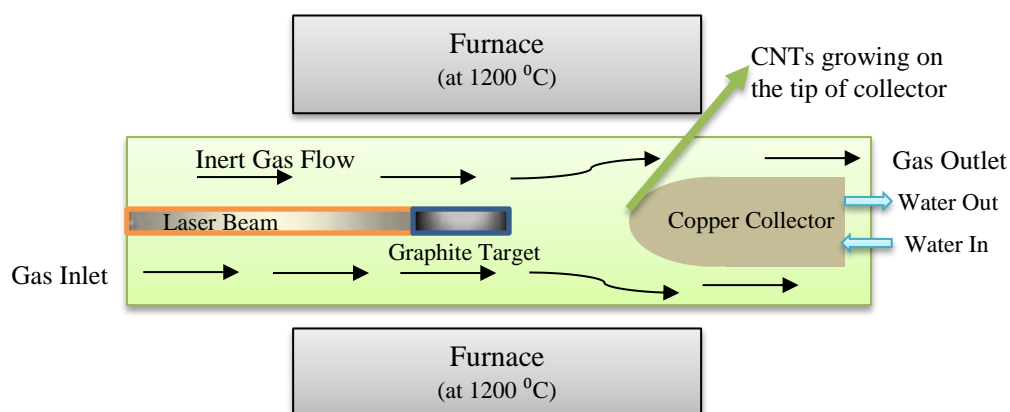


Figure 1: Experimental set up to produce CNTs by Laser ablation method. Reproduced with permission from ref. [38], M. M. A. Rafique and J. Iqbal, *J. Encapsulation Adsorpt. Sci.* 1, 29 (2011). Copyright@ Scientific Research Publishing.

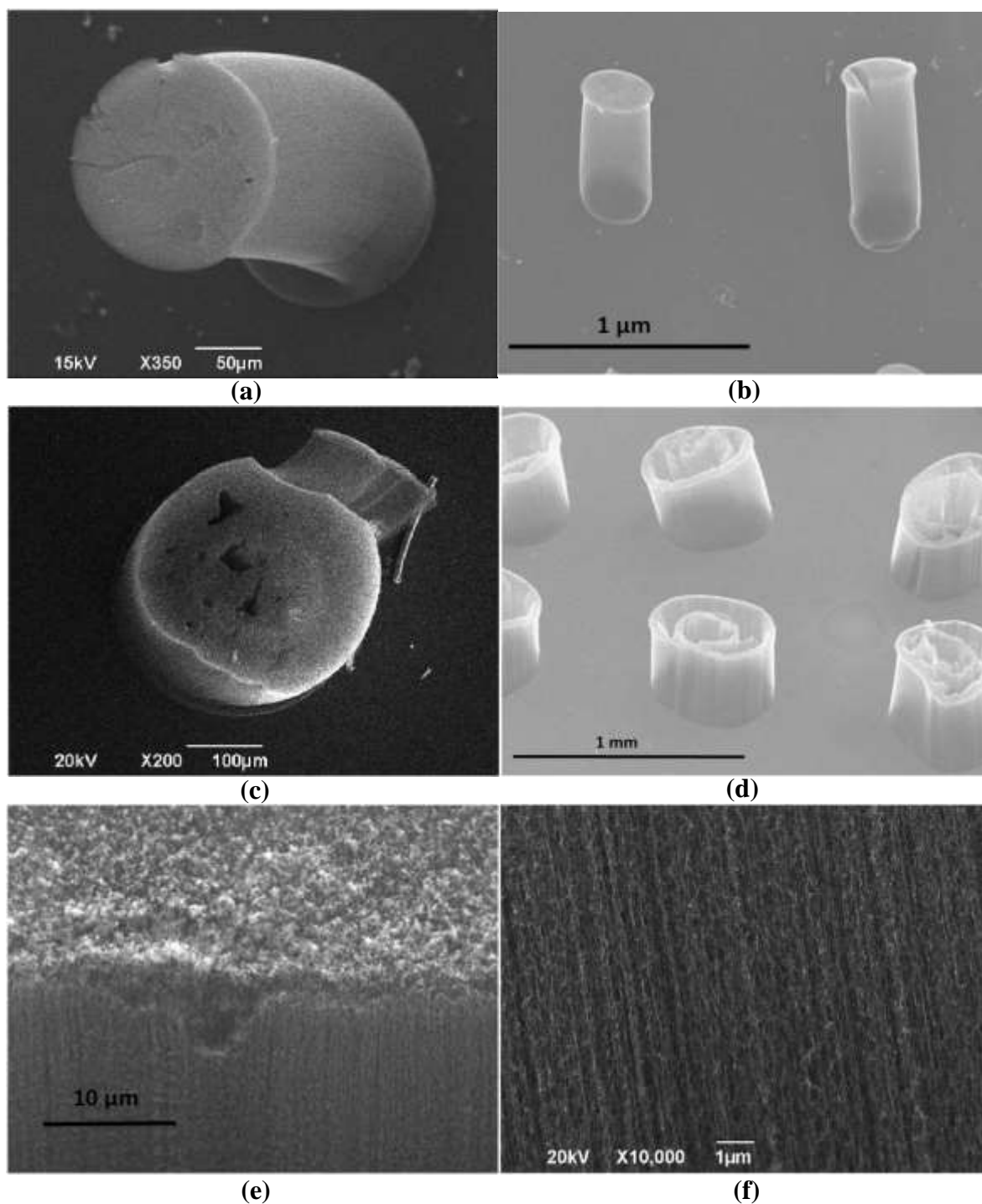


Figure 2. (a–d) SEM images of vertically aligned carbon nanotube forests localized at catalyst sites deposited by inkjet printing, using

(a) 1, (b) 8, (c) 27, (d) 64 drops/site. The 27- and 64-drop sites show less uniform growth than those grown with 1 and 8 drops/site, with vacancies within the nanotube forests. The forests in (d) show vertically aligned growth concentrated in concentric rings within the deposition site. These rings may arise due to the “coffee-ring” effect that produces non uniform distribution of catalyst particles within the printed region. (e) Magnified view of nanotube forest sidewall, from a forest grown using 64 drops/site of catalyst suspension, showing strong vertical alignment within the forest capped by a disordered “tangle” at the forest top. (f) Increased magnification image of forest sidewall, in this case from a forest grown using 27 drops/site, showing CNT alignment. Reprinted with permission from ref. [25], J. D. Beard, J. Stringer, O. R. Ghita, and P. J. Smith, *ACS Appl. Mater. Interfaces* 5, 9785 (2013). Copyright@ American Chemical Society.

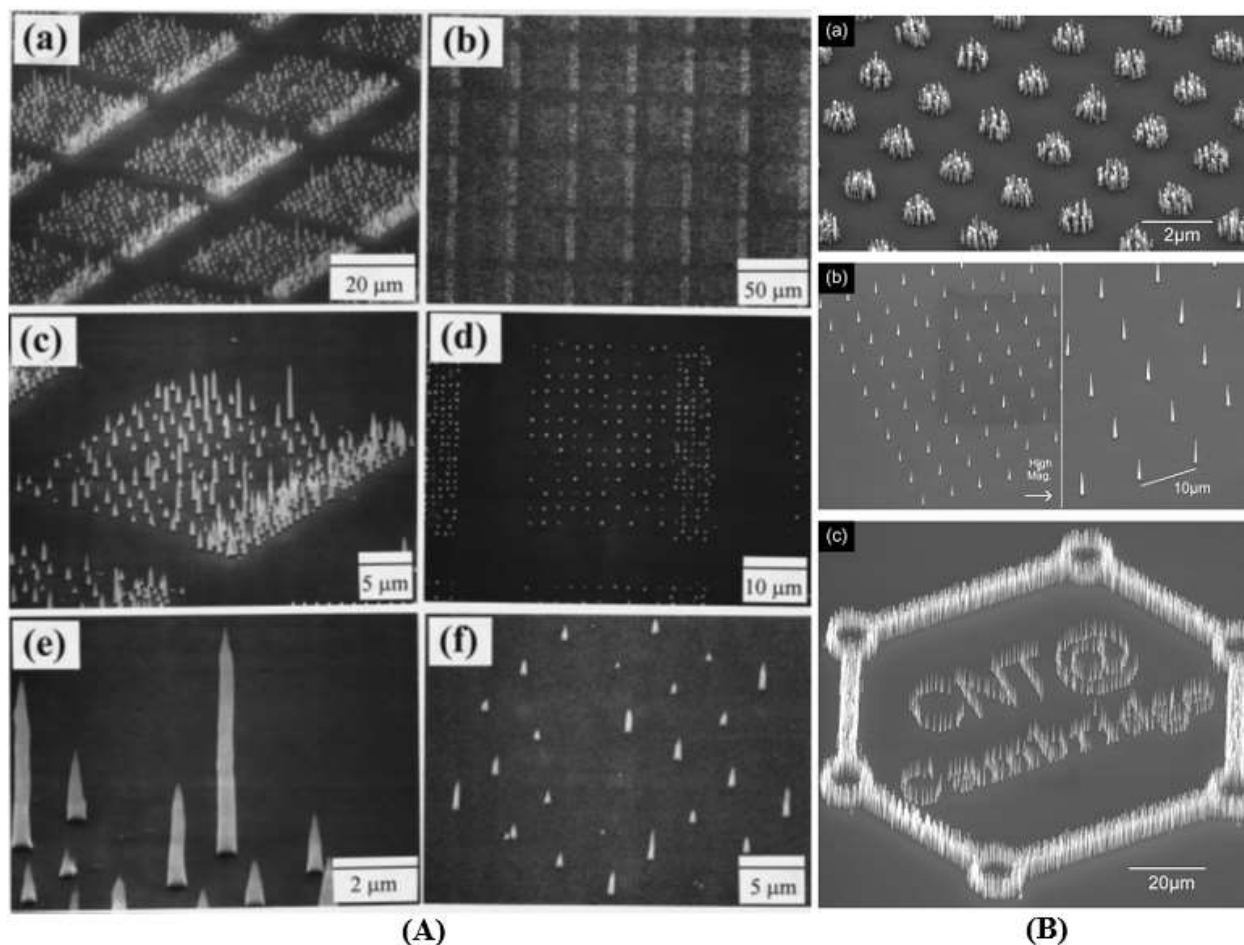


Figure 3. (A) A series of SEM micrographs from different viewing angles showing growth of carbon nanotube obelisks on an array of submicron nickel dots. (a) An inclined view of a repeated array pattern. (b) A top (normal) view of a repeated array pattern. (c) An inclined view of one array pattern. (d) A top (normal) view of one array pattern. The initial Ni dots (and subsequently the grown carbon structures) are spaced either 2 μm apart (left) or 1 μm apart (right). (e) A magnified view along the edge of one pattern. A sharp, tapered tip is evident. (f) An inclined view of carbon obelisks grown on nickel dots separated by 5 μm . Reprinted with permission from ref. [22]. F. Ren, Z.P. Huang, D.Z. Wang, J.G. Wen, J.W. Xu, J.H. Wang, L.E. Calvet, J. Chen, J.F. Klemic, M.A. Reed, *Appl. Phys. Lett.* 75, 1086 (1999). Copyright@ American Institute of Physics. (B) (a) Bunches of nanotubes (~ 100 nm in diameter) are deposited on 1 μm nickel dots because the nickel catalyst film breaks up into multiple nanoparticles. (b) Single nanotubes are deposited when the nickel dot size is reduced to 100 nm as only a single nickel nanoparticle is formed from the dot. (c) Demonstration of high yield, uniform, and selective growth of nanotubes at different densities. Reprinted with permission from ref. [175]. B.K. Teo, M. Chhowalla, G.A.I. Amaratunga, W.I. Milne, D.G. Hasko,

G. Pirio, P. Legagneux, F. Wyczisk, D. Pribat, *Appl. Phys. Lett.* 79, 1534 (2001).
Copyright@ American Institute of Physics.

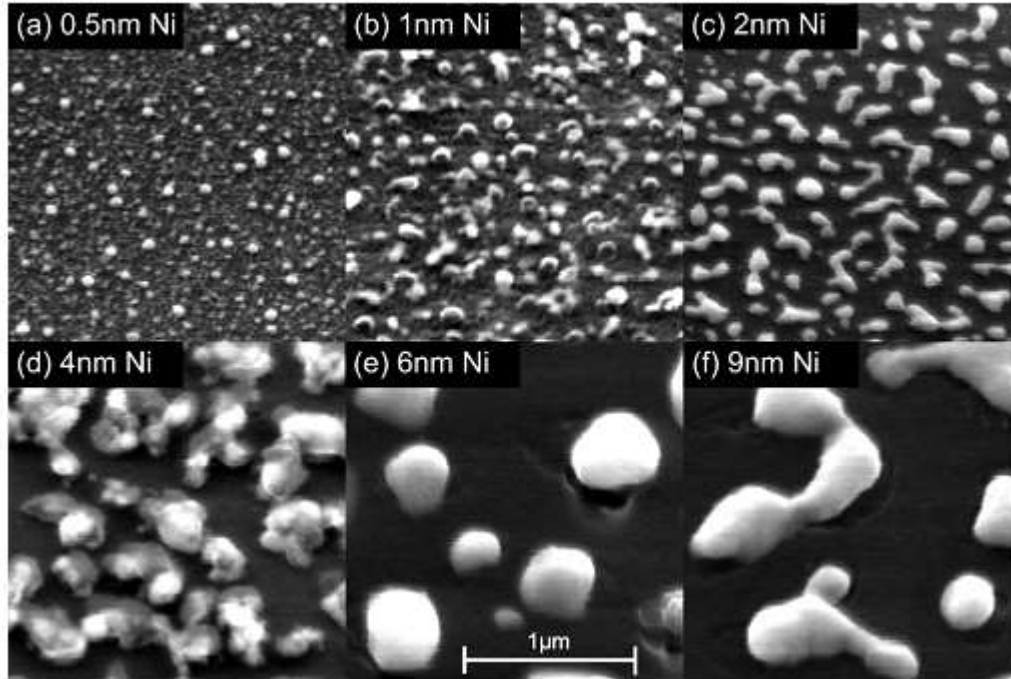


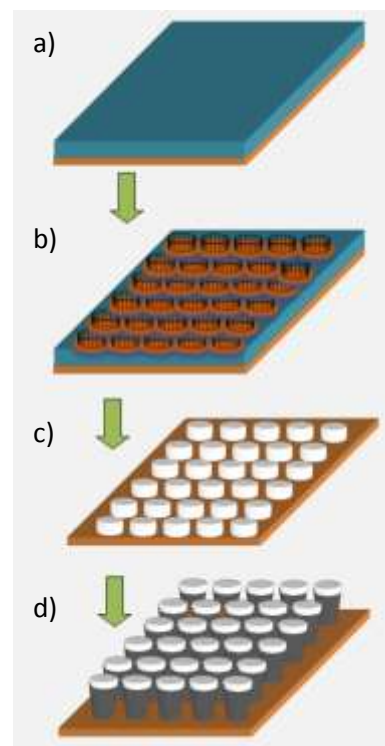
Figure 4: SEM images of Ni films with varying thicknesses deposited using magnetron sputtering on 50 nm of SiO₂ after annealing at 750 °C in 20 Torr of H₂ for 15 minutes. Reprinted with permission from ref. [124], M. Chhowalla, K. B. K. Teo, C. Ducati, N. L. Rupesinghe, G. a. J. Amaratunga, A. C. Ferrari, D. Roy, J. Robertson, and W. I. Milne, *J. Appl. Phys.* 90, 5308 (2001). Copyright@ American Institute of Physics.

Graphical Abstract

Synthesis of Patterned Vertically Aligned Carbon Nanotubes by PECVD using Different Growth Techniques: A Review

Aparna Gangele, Chandra Shekhar Sharma and Ashok Kumar Pandey

This review article gives a comprehensive analysis of the role of different key parameters responsible for the synthesis of the different structures and configurations of patterned vertical aligned carbon nanotubes, proposed in the last two decades and provides a critical analysis of the associated constraints, benefits, shortcomings and applications. The various methods of patterning and growing patterned VANCTs are also presented.



a) Photoresist/Substrate

b) Patterning by Photolithography

c) Catalyst Deposition and Lift off

d) CNTs growth by PECVD